

Historical and Future Weather Data for Dynamic Building Simulations in Belgium using the regional climate model MAR model: Typical & Extreme Meteorological Year and Heatwaves

5 Sébastien Doutreloup¹, Xavier Fettweis¹, Ramin Rahif², Essam Elnagar³, Mohsen S. Pourkiaei⁴, Deepak Amaripadath², Shady Attia²

¹: Laboratory of Climatology and Topoclimatology, Department de Geography, UR SPHERES, University of Liège, Belgium

²: Sustainable Building Design Lab, Dept. UEE, Faculty of Applied Sciences, University of Liege, Belgium

³: Thermodynamics Laboratory, Aerospace and Mechanical Engineering Department, Faculty of Applied Sciences, 10 University of Liège, Belgium

⁴: Atmospheres and Monitoring lab (SAM), UR Spheres, University of Liege, Arlon Campus Environment, Avenue de Longwy 185, 6700 Arlon, Belgium.

Correspondence to: Doutreloup S. (s.doutreloup@uliege.be)

Abstract. Increasing temperature due to global warming will influence building, heating and cooling practices. Therefore 15 this dataset aims to provide formatted and adapted meteorological data for specific users who work in building designing, architecture, building energy management systems, modelling renewable energy conversion systems, or other people interested in this kind of projected weather data. These meteorological data are produced from the regional climate model MAR (for “Modèle Atmosphérique Régional” in french) model simulations. This regional model adapted and validated over 20 Belgium is forced firstly by the ERA5 reanalysis which represents the closest climate to reality, and secondly by 3 ESMS from the – Sixth Coupled Model Intercomparison Project database, namely BCC-CSM2-MR, MPI-ESM.1.2, and MIROC6. The main advantage of using the MAR model is that the generated weather data have a high resolution (hourly data and 5km) and are spatially and temporally homogeneous. The generated weather data follow two protocols. On one hand, the 25 Typical Meteorological Year (TMY) and eXtreme Meteorological Year (XMY) files are generated largely inspired by the method proposed by the standard ISO15927-4, allowing the reconstruction of typical and extreme years while keeping a plausible variability of the meteorological data. On the other hand, the HeatWaves Event (HWE) meteorological data are generated according to a method used to detect the heatwave events and to classify them according to three criteria of the 30 heatwave (the most intense, the longest duration and the highest temperature). All generated weather data are freely available on the open online repository Zenodo (<https://doi.org/10.5281/zenodo.5606983> ; (Doutreloup, S. and Fettweis X., 2021)) and these data are produced within the framework of the research project OCCuPANT (<https://www.occupant.uliege.be/> - ULiège).

Keywords. Climate simulation; Future weather files; Typical year; Extreme year; Heatwave; Regional Modeling; Belgium

1 Introduction

On a global scale, the warmest (SSP5-8.5) scenario from the IPCC last assessment report (IPCC et al., 2021) suggests a temperature increase of +5°C by 2100. However, the regions of the world will not warm up at the same speed or intensity. Some regions, such as the poles, will warm faster and to higher levels than equatorial regions (Lee, J. Y. et al., 2021). Over the temperate ~~oceanic~~ regions such as Western Europe, the temperature is expected to increase between +1°C and +5°C in 2100 depending on the climate models and greenhouse gas emission scenarios used (Termonia et al., 2018; RMI, 2020; IPCC et al., 2021).

Moreover, IPCC et al. (2021) affirm that extreme events will become more probable and more intense. In particular, the maximum temperature is expected to increase faster (sometimes up to twice) than the mean temperature (Seneviratne, S. I. et al., 2021). Over Western-Central Europe, maximum temperatures are projected to increase up to +7°C for a global increase of +5°C (Seneviratne, S. I. et al., 2021).

More concretely, ~~duringin~~ the summer ~~season~~, hot extremes (including heatwaves) are already increasing and will continue to strengthen with global warming both in intensity and frequency (Suarez-Gutierrez et al., 2020; Seneviratne, S. I. et al., 2021; Dunn et al., 2020). The consequences of these heatwaves will affect human health (Fouillet et al., 2006), agriculture, the comfort and health of life inside buildings (Bruffaerts et al., 2018; Sherwood and Huber, 2010; Buysse et al., 2010), and the energy demand especially for cooling systems (Larsen et al., 2020). This is what motivated some previous studies in Belgium to represent the energy needs for heating and cooling under average and extreme weather conditions (Ramon et al., 2019).

The energy efficiency and living comfort are precisely what motivates the ULiège OCCuPANt project (Impacts Of Climate Change on the indoor environmental and energy PerformAnce of buildiNgS in Belgium during summer, <https://www.occupant.uliege.be/>) in which climate data are involved. **The OCCuPANt project aims to evaluate the energy performance and vulnerability of building inhabitants in the context of climate change. Acquiring reliable current and future climate data is vital in any study related to climate change and defines its quality (Pérez-Andreu and al., 2018).**

The purpose of this dataset is to propose meteorological data coming from a fine resolution regional climate model over Belgium and the neighbouring regions. These data will then be used to anticipate future climate changes which will influence both the production of heating and cooling demands as well as the electrical grids ~~on~~ in larger scales. These changes will require innovations in building design and systems which will necessarily take time. Thus, the more they are anticipated, the better we will find solutions. The use of a regional model allows building ~~of~~ spatially and temporally continuous and homogeneous past and future meteorological data according to different warming scenarios for some Belgian cities. This regional model is fed by the ERA-5 reanalysis model (Hersbach et al., 2020) to simulate the past climate (1980-2020) and also by 3 different Earth System Models (ESMs) from the Sixth Coupled Model Intercomparison Project (CMIP6) database

(Wu et al., 2019; Tatebe et al., 2019; Gutjahr et al., 2019) to obtain different future projections and associated uncertainties

65 for the same scenario SSP5-8.5.

The future climate data are very useful to predict the variations in heating and cooling demands in buildings. The characterization of minimum outdoor temperature under future scenarios is necessary to estimate the heating and cooling season needs. This can result in rethinking the building designs and making them resilient against the impact of climate change. For instance, in the heating-dominated region of Belgium, the concept of building design is more on heat retention to 70 decrease the heating energy use during the winter. However, by warming weather conditions in the last decades, such a design concept caused significant overheating problems during the summer. Therefore, it is necessary to predict the future performance of buildings and adapt them to the variations in the outdoor weather conditions. Designing cooling systems that can last for 100 years is challenging. However, it is possible to increase the preparedness of buildings to climate change 75 through passive design strategies, the use of active heating/cooling systems, or both. Both active and passive solutions may need regular replacements over the building life span.

For each city, considered period, model, and scenario, two synthetic files (in CSV format) are generated largely inspired by the method in ISO-15927-4: Typical Meteorological Year file (TMY) and eXtreme Meteorological Year file (XMY). In addition to these synthetic files, files focused on heatwaves are also generated, namely a file for the most intense heatwave event, one for the warmest heatwave, one for the longest heatwave, and one containing all the heatwaves detected within a 80 specific period. These files are described in detail in the methodology section.

2. Methodology

2.1 MAR model and area of interest

The regional climate model used in this study is the “Modèle Atmosphérique Régional” model (hereafter called “MAR”) in its version 3.11.4 (Kittel, 2021). The main role of MAR is to downscale a global model or reanalysis in order to get weather 85 outputs at a finer spatial and temporal resolution (Fig. 1). As shown in Fig. 1, MAR is a three-dimensional atmospheric model coupled to a one-dimensional transfer scheme between the surface, vegetation, and atmosphere (Ridder and Gallée, 1998). The MAR model also includes an urban island module which modifies the city grid points to simulate urban heat island through a modification of the surface albedo (fixed to 0.1) and an absence of vegetation which influence the thermal and humidity exchanges between soil and atmosphere. Initially, the MAR model was developed for both Greenland 90 (Fettweis et al., 2013) and Antarctica ice sheets (Agosta et al., 2019; Kittel et al., 2021). However, it has recently successfully adapted to temperate regions such as Belgium (Fettweis X. et al., 2017; Doutreloup et al., 2019; Wyard et al., 2021). In the framework of this study, MAR is initially forced every 6 hours at its lateral boundaries (temperature, wind, and specific humidity) by the reanalysis ERA5 (called hereafter MAR-ERA5) which is available at a horizontal resolution of ~31 km (Hersbach et al., 2020). Different kinds of observations (*in situ* weather observation, radar data, satellites, etc) are 6-

95 hourly assimilated into ERA5 to be the closest to the observed climate. In this way, the simulations of MAR-ERA5 can be considered as the closest simulation to the current observed climate.

Then, the MAR model has been forced every 6 hours by 3 ESMs from the CMIP6 database (Eyring et al., 2016). These ESMs do not contain any observational data and represent only an evolution of the average and interannual variability of the climatic parameters over long periods. These models contain two characteristic periods: one in the past, from 1980 to 2014 100 (hereafter called "historical" scenario), and another in the future, from 2015 to 2100 according to different SSP scenarios (SSP5-8.5, SSP3-7.0, and SSP2-4.5). The selection and description of each of these ESMs as well as a comparison with MAR-ERA5 over the historical period are presented in the next section.

The atmospheric variables used to force MAR every 6 hours at each vertical level are temperature, surface pressure, wind, and specific humidity, as well as the sea surface temperature over the North Sea from both ERA5 reanalysis (from 1980 to 105 2020) and the three ESMs (from 1980 to 2100). The spatial resolution of MAR is 5km over an integration domain (120 x 90 grid cells) centered over Belgium as shown in Fig. 2 to build hourly outputs.

The choice of 12 cities is motivated, on the one hand, by the size of the cities which must be sufficient to show a temperature increase compared to the neighbouring countryside and, on the other hand, to best represent climate spatial variability 110 observed in Belgium. For example, the city of Ostende is strongly influenced by the thermal inertia of the sea, while the city of Arlon has a more continental climate.

2.2 Forcing models and MAR simulations

2.2.1 Choice of representative Earth System Models

The Sixth Coupled Model Intercomparison Project (CMIP6; Eyring et al. (2016)) database contains about 30 ESMs from many scientific institutes around the world. For practical reasons, we can't regionalize all these ESMs. Thus, we had to 115 select a few representative ESMs for our region of interest, Western-Europe.

Our choice was based on two criteria. The first criterion is that the ESM should represent (with the lowest possible bias) the main atmospheric circulation in the free atmosphere over western Europe by evaluating the geopotential height at 500hPa and the temperature at 700hPa during summer and winter with respect to ERA5 over 1980-2014 based on the skill score 120 method developed by Connolley and Bracegirdle (2007). After selecting the ESMs that meet this first criterion, the second criterion is to choose 3 ESMs representing the CMIP6 models spread in 2100 for the same scenario (SSP5-8.5 here). Namely, we keep only 3 ESMs (see Tab. A1): BCC-CSM2-MR (Wu et al., 2019), MPI-ESM.1.2 (Gutjahr et al., 2019), and MIROC6 (Tatebe et al., 2019). The ESM BCC-CSM2-MR simulates a warming close to the ensemble mean of the 30 ESMs for the 2100 horizon using the SSP5-8.5 scenario, the ESM MIROC6 simulates a larger warming than the ensemble mean, and the ESM MPI-ESM.1.2 simulates a lower warming than the ensemble mean by 2100. The use of these 3 models allows 125 us to obtain a first approximation of the uncertainty from ESMs without having to downscale all the 30 available models of CMIP6.

2.2.2 Future ~~socioeconomics~~socio-economic scenarios

Shared Socio-economic Pathways (SSPs; Riahi et al. (2017)) are scenarios of global socio-economic evolution projected to 2100. These SSPs are used to develop greenhouse gas (~~GHG~~) emission (~~GHG~~) scenarios associated with different climate 130 policies and are used to force each future ESMs. There are 3 main scenarios, namely SSP2-4.5 (intermediate GHG), SSP3-7.0 (high GHG), and SSP5-8.5 (very high GHG), with their respectively increasingly warming for 2100. For more details about these scenarios, we refer to Riahi et al. (2017). Finally, it should be noted that the historical scenario mentioned in Section 2.1 is forced by the greenhouse gas concentrations observed over the period 1980-2014.

For the same practical reasons that led us to choose only 3 ESMs out of the 30 available models, we cannot afford to 135 calculate every SSP scenario of each ESM. Thus, since the ESMs do not simulate general atmospheric circulation changes (Eyring, V. et al., 2021) leading that only temperature drives the evolution of the climate. However, as the ESMs are not able to represent general circulation changes (Eyring, V. et al., 2021), the use of one scenario or another will not cause more blocking anticyclones leading to more persistent heatwaves for example. Thus, whichever scenario is used will only reflect temperature changes in relation to its GHG concentrations. Hence, only the SSP5-8.5 scenario has been calculated and the 140 other scenarios (SSP3-7.0 and SSP2-4.5) are derived from the MAR simulations forced by the ESMs using the SSP5-8.5 scenario since the warming rates from lower scenarios are included in the scenario SSP5-8.5 but for a different earlier time period. Thus, for each scenario (SSP3-7.0 and SSP2-4.5), the equivalent warming period in the SSP5-8.5 scenario has been found according to these 3 steps:

1) The raw 2m annual mean temperature of each ESM and each scenario has been aggregated over Belgium to the 145 horizon 2100;

2) For each ESM, the equivalent 20 years period from the SSP5-8.5 scenario has been chosen as the period with the closest mean and the closest interannual variability of the 2m annual temperature compared to the future 20 years period (i.e. 2021-2040, 2041-2060, ...) from the two other scenarios (SSP3-7.5 and SSP2-4.5);

3) Once the equivalent warming period has been identified, the data of this period is extracted out of the SSP5-8.5 150 forced MAR simulations for both SSP3-7.5 and SSP2-4.5 scenarios.

For example, the data of MAR-MPI for SSP3-7.0 over 2081-2100 are the outputs of MAR-MPI using SSP5-8.5 over the period 2066-2085.

This method is open to discussion for several reasons, firstly because the climate does not react in a linear way to an increase of GHG flowing through the different SSP scenarios. Moreover, with an equal warming rate but different periods, the Earth, 155 Atmosphere and Ocean systems will not have the same (spatial and temporal) responses due to their inertia. Despite these precautions, this methodology allows us on the one hand to derive a quick estimation without additional computer time. On the other hand, it remains valid as a first approximation, especially since the most interesting weather variable in this study is temperature, which is, by construction, the least sensitive to these issues. Hence, only the SSP5-8.5 scenario has been calculated to save computational time. Then, scenarios SSP3-7.0 and SSP2-4.5 are reconstructed from the MAR simulations

160 forced by the ESMs with the SSP5-8.5 scenario since the warning rates from the lower scenarios are included in this scenario SSP5-8.5 but for a different earlier period).—weather data of MAR-MPI with scenario SSP5-8.5 during the period 2066-2085 represent MAR-MPI with scenario SSP3-7.0 for the period 2081-2100 (i.e., the weather data of this corresponding period for SSP3-7.5 and SSP2-4.5 out of the SSP5-8.5 forced MAR simulations). Then, we extract Therefore, this method involves determining the period of the SSP5-8.5 scenario that corresponds to the warming rate projected by the other scenario for a given period. For this purpose, we use the raw data of each ESM and each scenario has been aggregated over Belgium to the horizon 2100. Then, for each ESM and for the SSP3-7.5 and SSP2-4.5 scenarios, we identify the corresponding period (the most equivalent mean and variability) in the SSP5-8.5 scenario.
165
170 This method is open to discussion for several reasons, firstly because climate does not react in a linear way to an increase of GHG flowing in different SSP scenarios. Moreover, with an equal warming rate but different periods, the Earth, Atmosphere and Ocean systems will not have the same (spatial and temporal) responses due to their inertia. Despite these precautions, the method used here allows on the one hand a very quick estimation without additional computer time. On the other hand, it remains valid as a first approximation, especially since the most interesting weather variable in this study is temperature, which is, therefore, the least sensitive to these issues.

2.2.3 Evaluation of the MAR simulations

175 To verify that these ESMs forced MAR simulations can be used to anticipate future periods, it is necessary to evaluate them over the present period over the overlapping period between the ERA5 reanalyses and the historical scenario (namely 1980-2014 which corresponds to the period of the historical scenario). The aim is to determine if they are able to represent the average and the climate variability over the Belgian territory for this period as observed (i.e. ERA5 in our case). So, we compare the 3 MAR simulations forced by the 3 ESMs with the MAR simulation forced by the ERA5 reanalyses. As in this ease, as the two the most important variables for this database are is the temperature at 2m above ground level (a.g.l.) and an important secondary variable is the incident incoming solar radiation, the mean and standard deviation of these data over the period 1980-2014 and over the Belgian territory are compared in Tab. 1 and Fig. 3. These values are compared on an annual scale as well as on a summer scale since the OCCuPANt project focuses on heatwaves.
180

185 The results of this comparison presented in Tab. 1 indicate that the incident incoming solar radiations and temperature at 2m a.g.l. values proposed by the 3 MAR simulations forced by the ESMs are mostly close to the average simulated by MAR-ERA5 with (not statistically significant) biases between MAR forced by the ESMs and MAR-ERA5 lower than the standard deviation (i.e. the interannual variability) of MAR-ERA5. We can also note that the interannual variability of the MAR simulations forced by the ESMs is close to the interannual variability of the MAR-ERA5 simulation. We can then conclude that the MAR simulations forced by the ESMs are able to represent the mean climate simulated by MAR-ERA5 and its 190 interannual variability with success, except MAR-MIR which significantly overestimates temperature and solar radiation in

summer. Knowing that MAR-MIR simulated the largest warming in 2100, this simulation needs to be considered as the extreme climate we could have.

2.3 Generating the ~~T~~ypical ~~M~~eteorological ~~Y~~ear and ~~e~~Xtreme ~~M~~eteorological ~~Y~~ear— files

The Typical Meteorological Year (TMY) and the eXtreme Meteorological Year (XMY) are datasets that are widely used by building designers and others for modelling renewable energy conversion systems (Wilcox and Marion, 2008). The TMYs are the synthetic years (on an hourly basis) constructed by representative typical months (Barnaby and Crawley, 2011) which are selected by comparing the distribution of each month within the long-term (minimum 10 years) distribution of that month for the available observations or modelled data (using Finkelstein-Schafer statistics (Finkelstein and Schafer, 1971). The XMY is the extension of the TMY weather data and is formed by selecting the most deviating (i.e., extreme) months over a certain dataset instead of typical months (Ferrari and Lee, 2008). There are many methods to reconstruct this kind of weather file (Ramon et al., 2019), but for this study, a protocol for the construction of these typical years has been developed based on the ISO15927-4 (European Standard, 2005) and is described briefly below.

The method consists of reconstituting each month of the typical (resp. extreme) year with the most typical (resp. extreme) month present in the considered period for a considered city. The comparison is essentially based on two variables, namely temperature at 2m a.g.l. and ~~incident~~incoming solar radiation. The choice of these two climatic parameters (~~called~~^{“para”}
~~hereafter~~) is related to the fact that they both influence the comfort inside the buildings. Therefore, we generate files with the typical year according to the temperature at 2m a.g.l. and, a typical year according to the ~~incident~~incoming solar radiation.

Here are the steps to find the most typical (resp. extreme) month for each ~~weather~~paraclimatic parameter:

1 Converting hourly file to daily file: From all the hourly data from all the same calendar months available within the selected period, the daily mean of ~~para~~the climatic parameter is computed;

2 Selecting the typical (extreme) month: For each calendar month, the percentile 50 (resp. 95) of ~~para~~the climatic parameter is calculated over the studied period to find the month which is the closest to the 50 percentile (resp. 95) of ~~para~~this climatic parameter;

3 Extracting hourly data of this typical (extreme) month: Finally, the hourly weather values of this typical (resp. extreme) month are stored in the file of the typical (resp. extreme) year.

The hourly weather variables available in the TMY and XMY files are described in Table 2.

1

2.4 Definition of a heatwave and generating the ~~h~~Heat~~W~~ave ~~e~~Event files

220 In Belgium, heatwaves are officially defined by two definitions, a retrospective one, and a prospective one. The retrospective heatwave is defined as periods of at least 5 consecutive days with a maximum temperature higher than 25°C, of which at

least 3 days within this period with a maximum temperature higher than 30°C (RMI, 2020). The prospective heatwave is a period with a predicted minimum temperature of 18.2°C or more and a maximum temperature of 29.6°C or higher both for 3 consecutive days (Tsachoua, L. and Reynders, D., 2016).

225 However, these definitions are static and do not consider the local climate of each region. For example, in the highlands (with altitudes above 300m in Figure 2) where it is on average colder, these heatwave criteria are not necessarily met, even though this region also experiences a heatwave. Moreover, when comparing the different ESMs, this fixed heatwave definition criterion could induce artefacts since each ESM has its own variability and biases over the current climate. For these reasons, we have used the statistical definition of a heatwave from (Ouzeau et al., 2016) computed for each MAR pixel 230 regardless of its basic climate, and each ESM independently of its own internal variability.

The calculation method, according to (Ouzeau et al., 2016), is as follows and it is illustrated in Fig. 4:

- For the period 1980-2014 (which corresponds to the "historical" scenario in the ESMs), for each pixel and each MAR simulation, we calculate three thresholds defined by 3 percentiles of the daily mean temperature: Sint = 95th percentile, Sdeb = 97.5th percentile and Spic = 99.5th percentile;
- A heatwave is detected when the daily mean temperature reaches Spic. The duration of this event is the number of days between the first day when the daily mean temperature is equal to or greater than Sdeb and either when the daily mean temperature falls below Sint or when the daily mean temperature falls below Sdeb for three consecutive days at least.
- In this dataset, we add a condition compared to (Ouzeau et al., 2016) which is that the minimum duration of the heatwave must be at least 5 consecutive days otherwise the heatwave event is not considered.

240 Once the heatwaves events (called "HWE" hereafter) are detected, we can characterize them according to three criteria:

- 1 the duration which is the number of consecutive days of the HWE;
- 2 the maximal daily mean temperature reached during the HWE;
- 3 the global intensity which is calculated by the cumulative difference between the temperature and the Sdeb threshold during the HWE, divided by the difference between Spic and Sdeb.

245 The hourly data provided in each HWE file are the same as for the TMY and XMY files (see section above). For each period, each city, each scenario, and each forcing, 4 files are created:

- a file containing hourly weather data for the longest HWE;
- a file containing the hourly weather data of the HWE characterized by the highest daily average temperature;
- a file containing the hourly weather data of the HWE characterized by the highest intensity;

250 ▪ a file that concatenates all the hourly weather data of all the HWEs present in a period, for each city, each scenario, and each MAR model.

Finally, the HWE files contain only the period corresponding to a heatwave event. However, depending on the purpose of the users, the effects of a heatwave can also be dependent on the period preceding and/or following it (depending on the use of the files and the purpose of the users). Thus, a suggestion for users could be to combine HWE files with files of typical or

255 extreme years in order to obtain simulations of a normal year with one or more heatwaves. We have not built these files in

order to leave it up to the users to combine or not these files and to prepare them according to their own constraints and interests.

3. The dataset

3.1 Data availability

260 The data described in this manuscript can be freely accessed on the Zenodo open-access repository: <https://doi.org/10.5281/zenodo.5606983> (Doutreloup, S. and Fettweis X., 2021). As the files are numerous, each zipped folder contains all the data for each city concerned by this dataset.

3.2 Structure of each file

All files are in CSV format comma-separated. The file names are formatted in such a way that they contain all the 265 information about the origin of the file. Each file name is composed as follows:

- | - For TMY or XMY: CityName_Type_Period_Scenario_MARmodel_ClimaticParameter.csv
- | - For Heatwave: CityName_Type_Period_Scenario_MARmodel.csv

with :

- CityName: the name of the city considered in this file;
- Type: the nature of this file, namely TMY (typical meteorological year), XMY (extreme meteorological year), HWE-HI (most intense heatwave event), HWE-HT (warmest heatwave event), HWE-LD (longest heatwave event), and HWE-all (all heatwave events);
- Period: the time period considered;
- Scenario: the IPCC scenario of the ESM considered, namely "hist", "SSP5-8.5", "SSP3-7.0", and "SSP2-4.5" (note 275 that for MAR-ERA5 the name of the scenario is set by default to "hist" even if the ERA5 forcing does not contain any scenario);
- MAR model: the version of MAR used, namely: MAR-ERA5, MAR-BCC, MAR-MPI or MAR-MIR;

| - **Para: is the climatic parameter used to generate the TMY or XMY file, namely the temperature at 2m a.g.l. (TT) or the incident solar radiation (SWD).**

280 For TMY and XMY files, the header is composed of the task number (which is a reference number for internal use in the OCCuPAnT project), the name of the city, and the name of the different variables accompanied by their unit. For HWE files, the header is composed of the task number (same remark as above), the name of the city, the characterization of the heatwave (longest, warmest, and most intense) accompanied by its period, and the name of the different variables accompanied by their unit. Then comes the weather data with the time variable in the first column. Weather data are in 285 universal time and leap year mode for the MAR-ERA5 and in no-leap year mode for MAR-BCC, MAR-MPI, and MAR-MIR.

A short example of how to select the desired data and files, as well as an example of how to use it, is provided in Appendix A for Liege-City.

4. Conclusion

290 The goal of this dataset is to provide formatted and adapted meteorological data for specific users who work in building
designing, architecture, building energy management systems, modelling renewable energy conversion systems, or other
people interested in this kind of data. These weather data are derived from the regional climate MAR model. This regional
model adapted and validated over Belgium is forced by a reanalysis and 3 ESMs. On one hand, MAR is forced by the ERA5
reanalysis to represent the closest climate to reality. On the other hand, MAR is forced by 3 ESMs from the CMIP6 database,
295 namely BCC-CSM2-MR, MPI-ESM.1.2, and MIROC6. The main advantage of using the MAR model is that the generated
weather data at high resolution are spatially and temporally homogeneous.

The generated weather data follow two protocols. Firstly, the TMY and XMY meteorological data are generated largely
inspired by the method proposed by the standard ISO15927-4, allowing the reconstruction of typical and extreme years while
300 keeping the plausible variability of the meteorological data. Secondly, the meteorological data concerning heatwaves (HWE)
are generated according to the method proposed by Ouzeau et al. (2016) to detect the heatwave events and classify them
according to three criteria of the heatwave. The OCCuPANT project, in which this paper is included, aims to identify the
highest temperature, the longest heatwave duration, and the most intense heatwave event. Finally, all generated weather data
are open source and freely available on the open repository Zenodo (<https://doi.org/10.5281/zenodo.5606983> ; (Doutreloup,
305 S. and Fettweis X., 2021).

5 Appendices

5.1 Appendix A: Example for Liege city

The Liege folder contains 596 files. This is a huge amount of files, so to find your way around we suggest the

following method for TMY and XMY files:-

310 1 Choosing a typical or extreme year, i.e. select XMY for an extreme year;
2 Choosing the parameter that determines the typical or extreme year (TT for temperature and SWD for
incidentincoming solar radiation), i.e. if you want a year with extreme incidentincoming solar radiation (i.e. sunshine), you
should select SWDbased.
3 Choosing the reference period, i.e. 2085-2100 for the end of the century;
315 4 Choosing the socio-economic scenario, i.e. "ssp585" for a world that continues to use fossil fuels;
5 Choosing one of the 3 MAR models, i.e. MAR-BCC for the MAR model forced by BCC-CSM2-MR;
6 Finally, the choice is made for the file:

Liege-City_XMY2085-2100_ssp585_MAR-BCC_SWDbased.csv

320 This file selection method is a proposal but each user is free to develop his own method and of course, youthe user can use several files to compare them. For example, if wethe user want to compare typical and extreme temperatures for the end of the century and for the two selected parameters with MAR-BCC, wethe user get Fig. A-1. Fig. A-1 which clearly shows that the extreme year temperature based on temperature is much higher than the typical year temperature. On the other hand, the extreme year temperature based on incidentincoming solar radiation is much lower, especially in January, than the typical year temperature because extreme radiation in winter usually means cold weather.

325 The method is almost identical for the heatwave files except that there are no parameters to determine the typical and extreme years but wethe user haves to choose if wehe want to look at the longest, the most intense, the hottest, or all heatwaves present within the period. Therefore, if wethe user want to compare the longest heatwave (HWE-LD) over the same period, for the same model and scenario as the example above, wethe user choose the file:-

Liege-City_HWE-LD_2085-2100_ssp585_MAR-BCC.csv

330 Fig. A-2 compares the temperature evolution during the warmest heatwave obtained from each of the MAR-BCC, MAR-MPI, and MAR-MIR simulations. The header of each file shows the warmest daily average temperature, namely 37.2°C for MAR-BCC, 35.3°C for MAR-MPI, and 37.8°C for MAR-MIR. However, it can be seen in Fig. A-2 that the hourly temperatures obviously rise much higher than these daily average values and in this case rise to ~44°C for MAR-BCC and 335 MAR-MIR and ~42°C for MAR-MPI.

6 Author contribution

All authors participated in the conceptualization of this paper. SD and XF designed the experiments and methodology and SD carried them out. SD prepared and created figures and data. XF oversaw the research. SD wrote the initial manuscript and all authors participated in the revision.

340 7 Competing interests

The authors declare that they have no conflict of interest.

8 Acknowledgment

This research was partially funded by the Walloon Region under the call “Actions de Recherche Concertées 2019 (ARC) and the project OCCuPANT, on the Impacts Of Climate Change on the indoor environmental and energy PerformAnce of 345 buildiNgs in Belgium during summer. The authors would like to gratefully acknowledge the Walloon Region and Liege University for funding. Computational resources have been provided by the Consortium des Équipements de Calcul Intensif

(CÉCI), funded by the Fonds de la Recherche Scientifique de Belgique (F.R.S.-FNRS) under Grant No. 2.5020.11 and by the Walloon Region.

9 Financial support

350 This research was partially funded by the Walloon Region under the call “Actions de Recherche Concertées 2019 (ARC)” and the project OCCuPANt, on the Impacts Of Climate Change on the indoor environmental and energy PerformAnce of buildiNgS in Belgium during summer.

10 References

Agosta, C., Amory, C., Kittel, C., Orsi, A., Favier, V., Gallée, H., van den Broeke, M. R., Lenaerts, J. T. M., van Wessem, J. M., van de Berg, W. J., and Fettweis, X.: Estimation of the Antarctic surface mass balance using the regional climate model MAR (1979–2015) and identification of dominant processes, *The Cryosphere*, 13, 281–296, <https://doi.org/10.5194/tc-13-281-2019>, 2019.

Barnaby, C. S. and Crawley, U. B.: Weather data for building performance simulation, in: *Building Performance Simulation for Design and Operation*, Routledge, 2011.

360 Bruffaerts, N., De Smedt, T., Delcloo, A., Simons, K., Hoebelke, L., Verstraeten, C., Van Nieuwenhuyse, A., Packeu, A., and Hendrickx, M.: Comparative long-term trend analysis of daily weather conditions with daily pollen concentrations in Brussels, Belgium, *Int. J. Biometeorol.*, 62, 483–491, <https://doi.org/10.1007/s00484-017-1457-3>, 2018.

Buyssse, D. J., Cheng, Y., Germain, A., Moul, D. E., Franzen, P. L., Fletcher, M., and Monk, T. H.: Night-to-night sleep variability in older adults with and without chronic insomnia, *Sleep Med.*, 11, 56–64, <https://doi.org/10.1016/j.sleep.2009.02.010>, 2010.

Connolley, W. M.; Bracegirdle, T. J. An Antarctic assessment of IPCC AR4 coupled models. *Geophys. Res. Lett.* 2007, 34, L22505, doi:10.1029/2007GL031648.

Doutreloup, S. and Fettweis X.: Typical & Extreme Meteorological Year and Heatwaves for Dynamic Building Simulations in Belgium based on MAR model Simulations (version 1.0.0) [Data set], <https://doi.org/10.5281/zenodo.5606983>, 2021.

370 Doutreloup, S., Wyard, C., Amory, C., Kittel, C., Erpicum, M., and Fettweis, X.: Sensitivity to Convective Schemes on Precipitation Simulated by the Regional Climate Model MAR over Belgium (1987–2017), *Atmosphere*, 10, 34, <https://doi.org/10.3390/atmos10010034>, 2019.

Duffie, J. A. and Beckman, W. A.: *Solar Engineering of Thermal Processes*, John Wiley&Sons, Inc., Hoboken, New Jersey, 2013.

375 Dunn, R. J. H., Alexander, L. V., Donat, M. G., Zhang, X., Bador, M., Herold, N., Lippmann, T., Allan, R., Aguilar, E., Barry, A. A., Brunet, M., Caesar, J., Chagnaud, G., Cheng, V., Cinco, T., Durre, I., Guzman, R. de, Htay, T. M., Ibadullah, W. M. W., Ibrahim, M. K. I. B., Khoshkam, M., Kruger, A., Kubota, H., Leng, T. W., Lim, G., Li-Sha, L., Marengo, J.,

Mbatha, S., McGree, S., Menne, M., Skansi, M. de los M., Ngwenya, S., Nkrumah, F., Oonariya, C., Pabon-Caicedo, J. D., Panthou, G., Pham, C., Rahimzadeh, F., Ramos, A., Salgado, E., Salinger, J., Sané, Y., Sopaheluwakan, A., Srivastava, A., 380 Sun, Y., Timbal, B., Trachow, N., Trewin, B., Schrier, G. van der, Vazquez-Aguirre, J., Vasquez, R., Villarroel, C., Vincent, L., Vischel, T., Vose, R., and Yussof, M. N. B. H.: Development of an Updated Global Land In Situ-Based Data Set of Temperature and Precipitation Extremes: HadEX3, *J. Geophys. Res. Atmospheres*, 125, e2019JD032263, <https://doi.org/10.1029/2019JD032263>, 2020.

European Standard: EN ISO 15927-4:2005 Hygrothermal performance of buildings — calculation and presentation of 385 climatic data — Part 4: Hourly data for assessing the annual energy use for heating and cooling (ISO 15927-4:2005)

Eyring, V., Bony, S., Meehl, G. A., Senior, C. A., Stevens, B., Stouffer, R. J., and Taylor, K. E.: Overview of the Coupled Model Intercomparison Project Phase 6 (CMIP6) experimental design and organization, *Geosci. Model Dev.*, 9, 1937–1958, <https://doi.org/10.5194/gmd-9-1937-2016>, 2016.

Eyring, V., N.P. Gillett, K.M. Achuta Rao, R. Barimalala, M. Barreiro Parrillo, N. Bellouin, C. Cassou, P.J. Durack, Y., 390 Kosaka, S. McGregor, S. Min, O. Morgenstern, Y. Sun, and Eyring, V., N.P. Gillett, K.M. Achuta Rao, R. Barimalala, M. Barreiro Parrillo, N. Bellouin, C. Cassou, P.J. Durack, Y.: Human Influence on the Climate System., in: Climate Change 2021: The Physical Science Basis. Contribution of Working Group I to the Sixth Assessment Report of the Intergovernmental Panel on Climate Change [Masson-Delmotte, V., P. Zhai, A. Pirani, S.L. Connors, C. Péan, S. Berger, N. Caud, Y. Chen, L. Goldfarb, M.I. Gomis, M. Huang, K. Leitzell, E. Lonnoy, J.B.R. Matthews, T.K. Maycock, T. Waterfield, 395 O. Yelekçi, R. Yu, and B. Zhou (eds.)], 2021.

Ferrari, D. and Lee, T.: Beyond TMY: Climate data for specific applications, in: in Proceedings 3rd International Solar Energy Society conference—Asia Pacific region (ISES-AP-08), 12, 2008.

Fettweis, X., Franco, B., Tedesco, M., van Angelen, J. H., Lenaerts, J. T. M., van den Broeke, M. R., and Gallée, H., 400 Estimating the Greenland ice sheet surface mass balance contribution to future sea level rise using the regional atmospheric climate model MAR, *The Cryosphere*, 7, 469–489, <https://doi.org/10.5194/tc-7-469-2013>, 2013.

Fettweis X., Wyard C., Doutreloup S., and Belleflamme A.: Noël 2010 en Belgique: neige en Flandre et pluie en Haute-Ardenne, *Bull. Société Géographique Liège*, 68, 97–107, 2017.

Finkelstein, J. M. and Schafer, R. E.: Improved goodness-of-fit tests, *Biometrika*, 58, 641–645, <https://doi.org/10.1093/biomet/58.3.641>, 1971.

405 Fouillet, A., Rey, G., Laurent, F., Pavillon, G., Bellec, S., Guihenneuc-Jouyaux, C., Clavel, J., Jouglard, E., and Hémon, D.: Excess mortality related to the August 2003 heat wave in France, *Int. Arch. Occup. Environ. Health*, 80, 16–24, <https://doi.org/10.1007/s00420-006-0089-4>, 2006.

Gutjahr, O., Putrasahan, D., Lohmann, K., Jungclaus, J. H., von Storch, J.-S., Brüggemann, N., Haak, H., and Stössel, A., 410 Max Planck Institute Earth System Model (MPI-ESM1.2) for the High-Resolution Model Intercomparison Project (HighResMIP), *Geosci. Model Dev.*, 12, 3241–3281, <https://doi.org/10.5194/gmd-12-3241-2019>, 2019.

Hersbach, H., Bell, B., Berrisford, P., Hirahara, S., Horányi, A., Muñoz-Sabater, J., Nicolas, J., Peubey, C., Radu, R.,

415 Schepers, D., Simmons, A., Soci, C., Abdalla, S., Abellan, X., Balsamo, G., Bechtold, P., Biavati, G., Bidlot, J., Bonavita, M., Chiara, G. D., Dahlgren, P., Dee, D., Diamantakis, M., Dragani, R., Flemming, J., Forbes, R., Fuentes, M., Geer, A., Haimberger, L., Healy, S., Hogan, R. J., Hólm, E., Janisková, M., Keeley, S., Laloyaux, P., Lopez, P., Lupu, C., Radnoti, G., Rosnay, P. de, Rozum, I., Vamborg, F., Villaume, S., and Thépaut, J.-N.: The ERA5 global reanalysis, *Q. J. R. Meteorol. Soc.*, 146, 1999–2049, <https://doi.org/10.1002/qj.3803>, 2020.

420 IPCC, Masson Delmotte, V., P. Zhai, A. Pirani, S. L. Connors, C. Péan, S. Berger, N. Caud, Y. Chen, L. Goldfarb, M. I. Gomis, M., and Huang, K. Leitzell, E. Lonnoy, J. B. R. Matthews, T. K. Maycock, T. Waterfield, O. Yelekçi, R. Yu and B. Zhou: Summary for Policymakers. In: *Climate Change 2021: The Physical Science Basis. Contribution of Working Group I to the Sixth Assessment Report of the Intergovernmental Panel on Climate Change*, 2021.

Kittel, C.: Present and future sensitivity of the Antarctic surface mass balance to oceanic and atmospheric forcings: insights with the regional climate model MAR, PhD Thesis, Université de Liège, Liège, Belgique, Liège, 2021.

425 Kittel, C., Amory, C., Agosta, C., Jourdain, N. C., Hofer, S., Delhasse, A., Doutreloup, S., Huot, P.-V., Lang, C., Fichefet, T., and Fettweis, X.: Diverging future surface mass balance between the Antarctic ice shelves and grounded ice sheet, *The Cryosphere*, 15, 1215–1236, <https://doi.org/10.5194/tc-15-1215-2021>, 2021.

Larsen, M. A. D., Petrović, S., Radoszynski, A. M., McKenna, R., and Balyk, O.: Climate change impacts on trends and extremes in future heating and cooling demands over Europe, *Energy Build.*, 226, 110397, <https://doi.org/10.1016/j.enbuild.2020.110397>, 2020.

430 Lee, J. Y., J. Marotzke, G. Bala, L. Cao, S. Corti, J. P. Dunne, F. Engelbrecht, E. Fischer, J. C. Fyfe, C. Jones, A., and Maycock, J. Mutemi, O. Ndiaye, S. Panickal, T. Zhou: Future Global Climate: Scenario-Based Projections and Near-Term Information, Camb. Univ. Press, *Climate Change 2021: The Physical Science Basis. Contribution of Working Group I to the Sixth Assessment Report of the Intergovernmental Panel on Climate Change* [Masson-Delmotte, V., P. Zhai, A. Pirani, S. L. Connors, C. Péan, S. Berger, N. Caud, Y. Chen, L. Goldfarb, M. I. Gomis, M. Huang, K. Leitzell, E. Lonnoy, J. B. R. Matthews, T. K. Maycock, T. Waterfield, O. Yelekçi, R. Yu and B. Zhou (eds.)], 2021.

435 Ouzeau, G., Soubeyroux, J.-M., Schneider, M., Vautard, R., and Planton, S.: Heat waves analysis over France in present and future climate: Application of a new method on the EURO-CORDEX ensemble, *Clim. Serv.*, 4, 1–12, <https://doi.org/10.1016/j.cliser.2016.09.002>, 2016.

Pérez-Andreu V., Aparicio-Fernández C., Martínez-Ibernón A. and Vivancos J.-L.: Impact of climate change on heating and cooling energy demand in a residential building in a Mediterranean climate, *Energy*, vol. 165, pp. 63–74, Dec. 2018, doi: 440 10.1016/j.energy.2018.09.015.

Ramon, D., Allacker, K., van Lipzig, N. P. M., De Troyer, F., and Wouters, H.: Future Weather Data for Dynamic Building Energy Simulations: Overview of Available Data and Presentation of Newly Derived Data for Belgium, in: *Energy Sustainability in Built and Urban Environments*, edited by: Motoasca, E., Agarwal, A. K., and Breesch, H., Springer, Singapore, 111–138, https://doi.org/10.1007/978-981-13-3284-5_6, 2019.

445 Riahi, K., van Vuuren, D. P., Kriegler, E., Edmonds, J., O'Neill, B. C., Fujimori, S., Bauer, N., Calvin, K., Dellink, R.,

450 Fricko, O., Lutz, W., Popp, A., Cuaresma, J. C., Kc, S., Leimbach, M., Jiang, L., Kram, T., Rao, S., Emmerling, J., Ebi, K., Hasegawa, T., Havlik, P., Humpenöder, F., Da Silva, L. A., Smith, S., Stehfest, E., Bosetti, V., Eom, J., Gernaat, D., Masui, T., Rogelj, J., Strefler, J., Drouet, L., Krey, V., Luderer, G., Harmsen, M., Takahashi, K., Baumstark, L., Doelman, J. C., Kainuma, M., Klimont, Z., Marangoni, G., Lotze-Campen, H., Obersteiner, M., Tabeau, A., and Tavoni, M.: The Shared Socioeconomic Pathways and their energy, land use, and greenhouse gas emissions implications: An overview, *Glob. Environ. Change*, 42, 153–168, <https://doi.org/10.1016/j.gloenvcha.2016.05.009>, 2017.

Ridder, K. D. and Gallée, H.: Land Surface–Induced Regional Climate Change in Southern Israel, *J. Appl. Meteorol. Climatol.*, 37, 1470–1485, [https://doi.org/10.1175/1520-0450\(1998\)037<1470:LSIRCC>2.0.CO;2](https://doi.org/10.1175/1520-0450(1998)037<1470:LSIRCC>2.0.CO;2), 1998.

RMI: Rapport climatique 2020 de l’information aux services climatiques, Royal Meteorological Institute of Belgium, Brussels, 2020.

Seneviratne, S. I., Zhang X., M. Adnan, W. Badi, C. Dereczynski, A. Di Luca, S. Ghosh, I. Iskandar, J. Kossin, S., and Lewis, F. Otto, I. Pinto, M. Satoh, S. M. Vicente-Serrano, M. Wehner, B. Zhou: Weather and Climate Extreme Events in a Changing Climate, *Clim. Change* 2021 Phys. Sci. Basis Contrib. Work. Group Sixth Assess. Rep. Intergov. Panel Clim. Change Masson-Delmotte V P Zhai Pirani Connors C Péan Berg. N Caud Chen Goldfarb M Gomis M Huang K Leitzell E Lonnoy J B R Matthews T K Maycock T Waterfield O Yelekçi R Yu B Zhou Eds, 2021.

Sherwood, S. C. and Huber, M.: An adaptability limit to climate change due to heat stress, *Proc. Natl. Acad. Sci.*, 107, 9552–9555, <https://doi.org/10.1073/pnas.0913352107>, 2010.

Suarez-Gutierrez, L., Müller, W. A., Li, C., and Marotzke, J.: Hotspots of extreme heat under global warming, *Clim. Dyn.*, 55, 429–447, <https://doi.org/10.1007/s00382-020-05263-w>, 2020.

465 Tatebe, H., Ogura, T., Nitta, T., Komuro, Y., Ogochi, K., Takemura, T., Sudo, K., Sekiguchi, M., Abe, M., Saito, F., Chikira, M., Watanabe, S., Mori, M., Hirota, N., Kawatani, Y., Mochizuki, T., Yoshimura, K., Takata, K., O’ishi, R., Yamazaki, D., Suzuki, T., Kurogi, M., Kataoka, T., Watanabe, M., and Kimoto, M.: Description and basic evaluation of simulated mean state, internal variability, and climate sensitivity in MIROC6, *Geosci. Model Dev.*, 12, 2727–2765, <https://doi.org/10.5194/gmd-12-2727-2019>, 2019.

470 Termonia, P., Van Schaeybroeck, B., De Cruz, L., De Troch, R., Caluwaerts, S., Giot, O., Hamdi, R., Vannitsem, S., Duchêne, F., Willems, P., Tabari, H., Van Uytven, E., Hosseinzadehtalaei, P., Van Lipzig, N., Wouters, H., Vanden Broucke, S., van Ypersele, J.-P., Marbaix, P., Villanueva-Birriel, C., Fettweis, X., Wyard, C., Scholzen, C., Doutreloup, S., De Ridder, K., Gobin, A., Lauwaet, D., Stavrakou, T., Bauwens, M., Müller, J.-F., Luyten, P., Ponsar, S., Van den Eynde, D., and Pottiaux, E.: The CORDEX.be initiative as a foundation for climate services in Belgium, *Clim. Serv.*, 11, 49–61, <https://doi.org/10.1016/j.cliner.2018.05.001>, 2018.

Tsachoua, L. and Reynders, D.: Hittegolf en Ozonpiekenplan, https://www.belspo.be/belspo/organisation/publ/pub_ostc/agora/ragjj146_en.pdf, 2016.

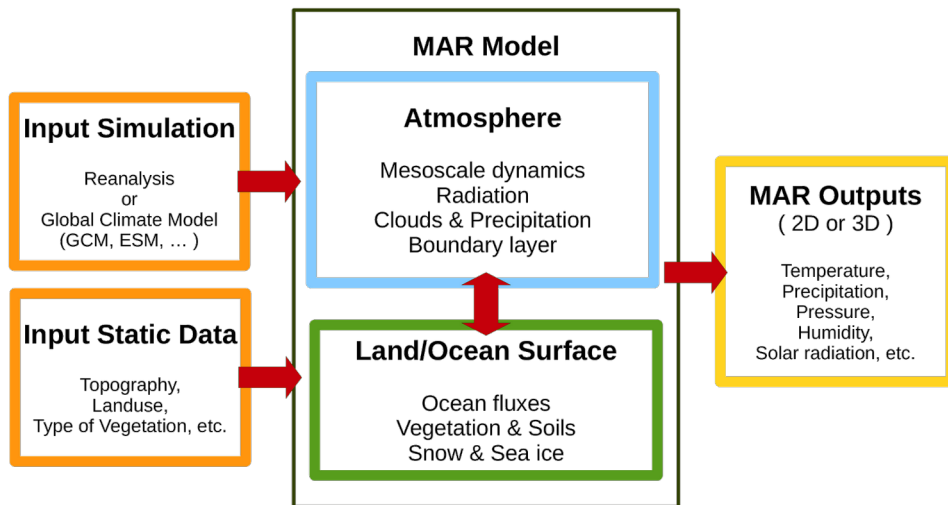
Wilcox, S. and Marion, W.: Users Manual for TMY3 Data Sets, 2008.

Wu, T., Lu, Y., Fang, Y., Xin, X., Li, L., Li, W., Jie, W., Zhang, J., Liu, Y., Zhang, L., Zhang, F., Zhang, Y., Wu, F., Li, J.,

480 Chu, M., Wang, Z., Shi, X., Liu, X., Wei, M., Huang, A., Zhang, Y., and Liu, X.: The Beijing Climate Center Climate System Model (BCC-CSM): the main progress from CMIP5 to CMIP6, *Geosci. Model Dev.*, 12, 1573–1600, <https://doi.org/10.5194/gmd-12-1573-2019>, 2019.

Wyard, C., Scholzen, C., Doutreloup, S., Hallot, É., and Fettweis, X.: Future evolution of the hydroclimatic conditions favouring floods in the south-east of Belgium by 2100 using a regional climate model, *Int. J. Climatol.*, 41, 647–662,

485 <https://doi.org/10.1002/joc.6642>, 2021.



490 **Figure 1: Workflow of the MAR model.** The MAR model (black box) needs to be forced by a reanalysis model or global model (upper orange box) and by static data (lower orange box) and the result of the MAR simulation gives meteorological variables in two or three dimensions (yellow box).

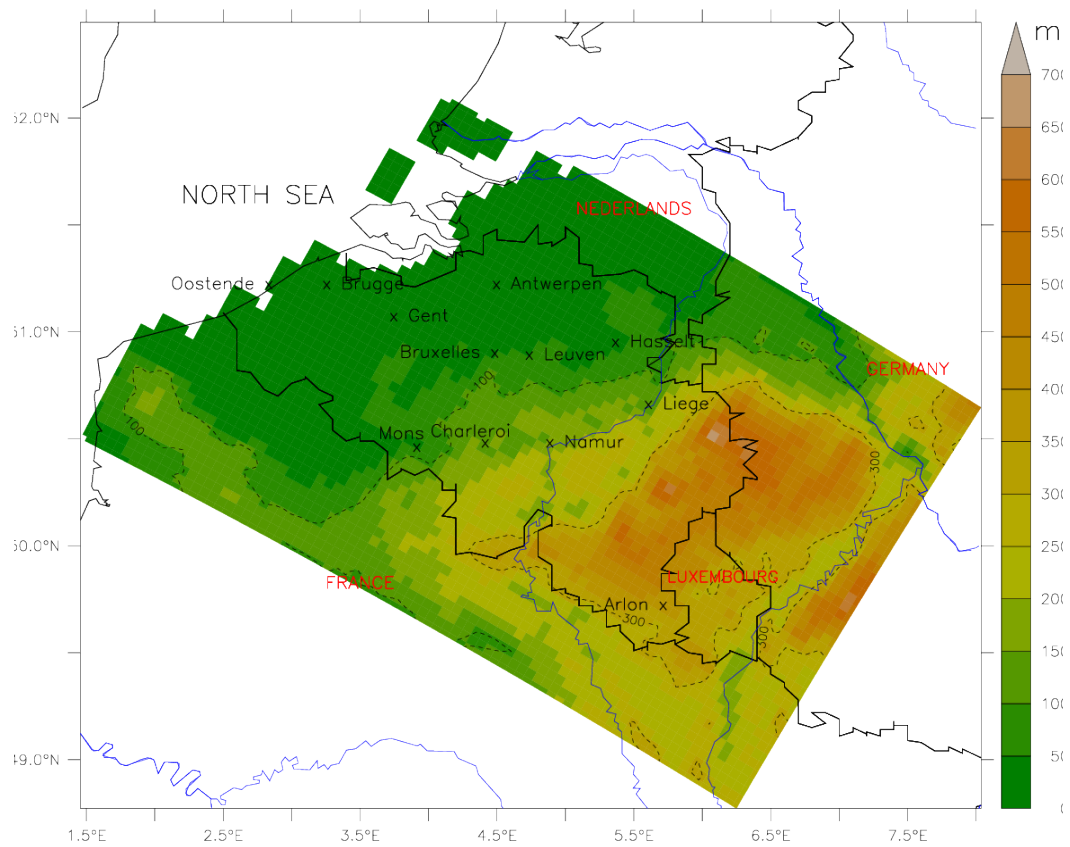
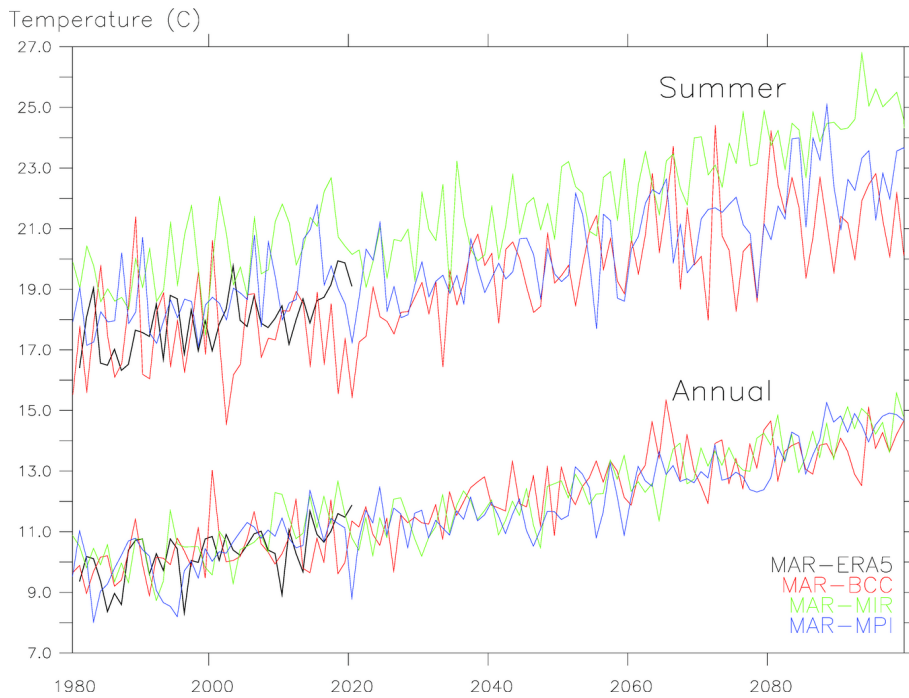
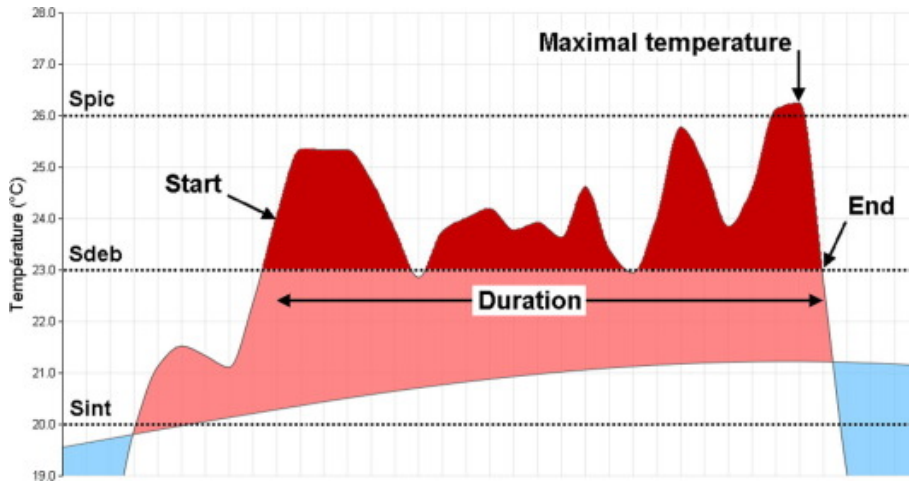


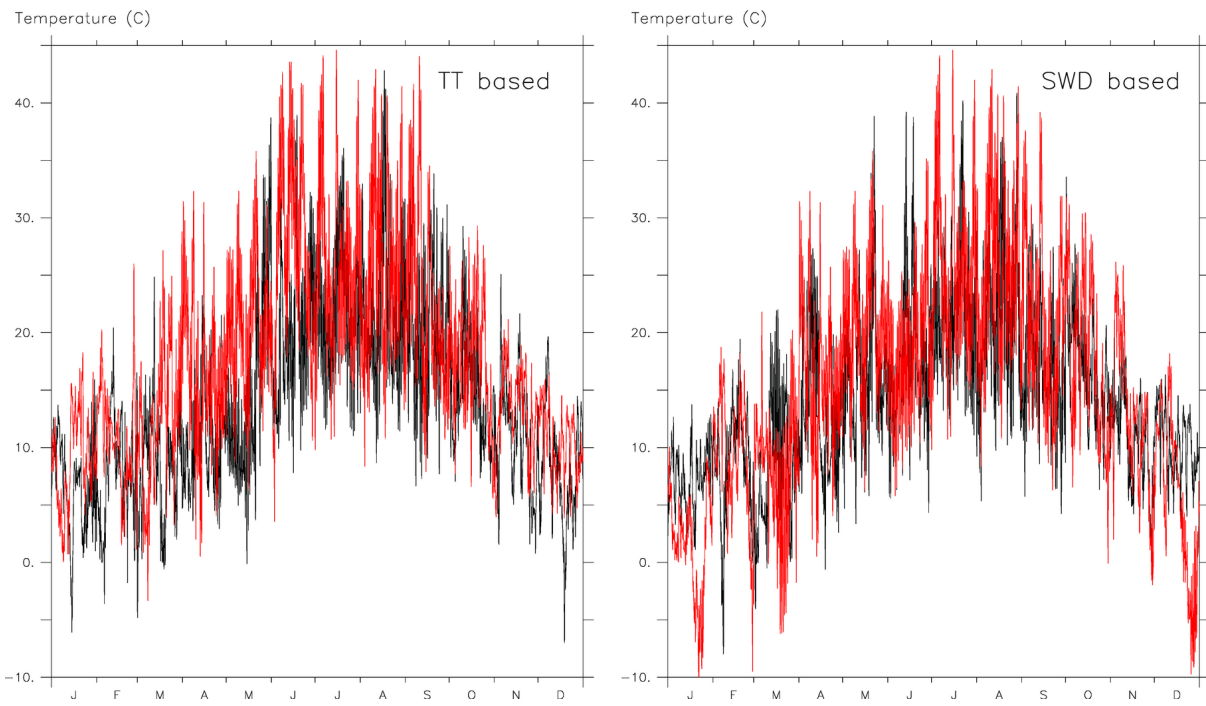
Figure 2: Model topography (colour background, in meters and dashed black line, both in meters above sea level), localization of cities (black letters) used in this dataset for Belgium, and localization of neighbouring countries (in red letters).



495 **Figure 3: Annual mean temperature (in C, lower lines) and annual summer temperature (in C, upper lines) of MAR forced by ERA5 reanalysis (in black bold lines), MAR-BCC (i.e., MAR forced by BCC-CSM2-MR; in red lines), MAR-MPI (i.e., MAR forced by MPI-ESM1.2 ; in blue lines), and MAR-MIR (i.e., MAR forced by MIROC6 ; in green lines) between 1980 and 2100 according to the scenario SSP5-8.5. The average is computed here over the whole integration domain excluding the ocean.**

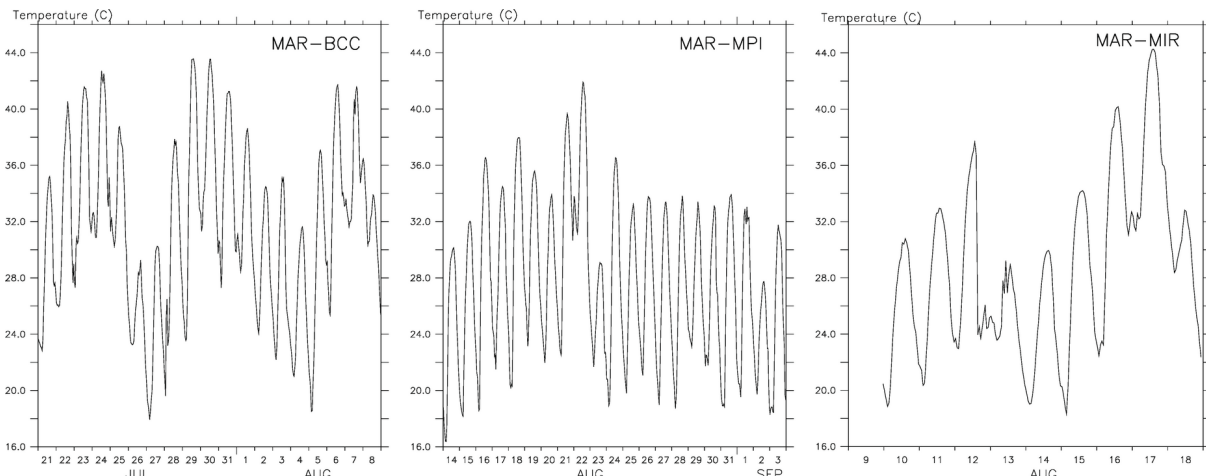


500 **Figure 4 (figure and legend coming from Ouzeau et al., 2016): Characterization of a heatwave from a daily mean temperature indicator over France (example of a time series from June 30 to August 5, 1983): Duration (start and end), maximal temperature, and global intensity (red area of the plot). Temperatures above (below) climatological line (1981–2010 reference period) are represented by the pink (blue) area. (For interpretation of the references to colour in this figure legend, the reader is referred to the web version of this article.)**



505 | **Figure A-1:** Typical (black) and extreme (red) temperature for Liege city simulated by MAR forced by BCC-CSM2-MR with the scenario SSP5-8.5 for the period 2085-2100. The typical/extreme months are based on temperature (left) and [incident/incoming](#) solar radiation (right). These data are extracted from these files :

510 | - Liege-City_TMY2085-2100_ssps585_MAR-BCC_TTbased.csv
 - Liege-City_XMY2085-2100_ssps585_MAR-BCC_TTbased.csv
 - Liege-City_TMY2085-2100_ssps585_MAR-BCC_SWDbased.csv
 - Liege-City_XMY2085-2100_ssps585_MAR-BCC_SWDbased.csv



515 | **Figure A-2:** Temperature during warmest heatwave events for Liege city simulated by MAR-BCC (i.e., MAR forced by BCC-CSM2-MR), MAR-MPI (i.e., MAR forced by MPI-ESM.1.2), and MAR-MIR (i.e., MAR forced by MIROC6) with the scenario SSP5-8.5 for the period 2085-2100. These data are extracted from these files :

- Liege-City_HWE-HT_2085-2100_ssps585_MAR-BCC.csv

1980-2014 over Belgium territory	Time scale	MAR-ERA5	MAR-BCC	MAR-MPI	MAR-MIR
Mean temperature at 2m a.g.l. (in C)	annual	10.1 +/- 6.2	10.3 +/- 6.0	10.1 +/- 6.4	10.4 +/- 7.2
	summer	17.7 +/- 1.3	17.6 +/- 1.7	18.6 +/- 1.2	19.9 +/- 1.1
Mean <u>incident</u> <u>incoming</u> solar radiation (in W/m ²)	annual	119 +/- 78	122 +/- 79	116 +/- 83	134 +/- 85
	summer	213 +/- 20	221 +/- 20	224 +/- 22	239 +/- 25

Table 1: Comparison of MAR-ERA5 (i.e., MAR forced by the reanalysis ERA5) with MAR-BCC (i.e., MAR forced by BCC-CSM2-MR), MAR-MPI (i.e., MAR forced by MPI-ESM.1.2), and MAR-MIR (i.e., MAR forced by MIROC6) to mean temperature at 2m above ground level and mean incidentincoming solar radiation over Belgium territory during 1980-2014 (mean value +/- standard error).

Weather variable name	Level	Units
Dry bulb temperature	2m a.g.l.	°C
Relative humidity	2m a.g.l.	%
Global horizontal radiation	Ground (horizontal surface)	Wh/m ²
Diffuse solar radiation	Ground (horizontal surface)	Wh/m ²
Direct normal radiation	Ground (horizontal surface)	Wh/m ²
Wind speed	10m a.g.l.	m/s
Wind direction	10m a.g.l.	north degrees
Dew point temperature	2m a.g.l.	°C
Atmospheric Pressure	ground	Pa
Cloudiness	All troposphere	tenths
Sky temperature	All troposphere	K
(according to (Duffie and Beckman, 2013))		
Specific humidity	2m a.g.l.	kg/kg
Precipitation	Ground	mm

Table 2: name, level and units of all weather variables used in the produced weather files.

Full name of the ESM	Abbreviation name of the ESM	Lead institution	References

<u>BCC-CSM2-MR</u>	<u>BCC</u>	<u>Beijing Climate Centre</u>	<u>(Wu et al., 2019)</u>
<u>MPI-ESM1-2-HR</u>	<u>MPI</u>	<u>Max Planck Institute</u>	<u>(Gutjahr et al., 2019)</u>
<u>MIROC6</u>	<u>MIR</u>	<u>Japanese modelling community</u>	<u>(Tatebe et al., 2019)</u>

Table A1: full name, abbreviation name, lead institution and references of the Earth System Model (ESM) used in this study.

530